PHYSICAL REVIEW E **76**, 020901(R) (2007)

Quantized cycling time in artificial gene networks induced by noise and intercell communication

Aneta Koseska,[1] Evgenii Volkov,[2] Alexei Zaikin,[3] and Jürgen Kurths[1]
[1]*Institut für Physik, Potsdam Universität, Am Neuen Palais 10,D-14469 Potsdam, Germany*
[2]*Department of Theoretical Physics, Lebedev Physical Institute, Leninskii 53, Russia*
[3]*Department of Mathematics, University of Essex, Wivenhoe Park, Colchester C04 3SQ, United Kingdom*
(Received 9 March 2007; revised manuscript received 23 July 2007; published 23 August 2007)

We propose a mechanism for the quantized cycling time based on the interplay of cell-to-cell communication and stochasticity, by investigating a model of coupled genetic oscillators with known topology. In addition, we discuss how inhomogeneity can be used to enhance such quantizing effects, while the degree of variability obtained can be controlled using the noise intensity or adequate system parameters.

DOI: 10.1103/PhysRevE.76.020901 PACS number(s): 87.18.−h, 05.40.Ca, 05.45.Xt

The idea of a quantized generation time occupies a significant place in research into time-dependent biological processes, e.g., in cell cycle research [1]. Clear experimental evidence for quantized cycles has been obtained for Chinese hamster *V*79 cells [2], *wee*1$^-$*cdc*25Δ fission yeast cells [3], *Xenopus oocytes* [4], etc. Quantized cycling is the name commonly used when a basic dynamical property of a homogeneous system demonstrates a clear multipeak character instead of a flat distribution. Manifestations of this effect are, e.g., the multimodal interspike interval probability density in neurons [5,6], or the polymodal distribution of intermitotic times in proliferating cell cultures [1]. To our knowledge, two mechanisms are mainly responsible for the quantized dynamical behavior in biological systems. The first mechanism considers the interplay of external forcing, nonlinearity, and stochasticity in the system as a determining reason [6], an idea reminiscent of the effect of stochastic resonance [7] (there are reports as well where an internal oscillator plays the role of a periodic force [2]). The second mechanism is based on the complex structure of the phase space disturbed by noise [8,9]. It is important to note that these mechanisms are based on the properties of a single, noncoupled oscillator under the influence of forcing.

It is a well-established fact, however, that cells are organized in large populations, exchanging information in a stochastic environment through different types of intercell communication mechanism. Hence, the additional question naturally arises as to whether intercell coupling can provide the necessary background for quantized cycling due to noise. Relying on this assumption, we propose here a different mechanism for quantized cycling generation, which relies on the interplay between noise and the complex behavior of the dynamical system induced by specific, inhibitory, phase-repulsive intercell coupling, and discuss a strategy to control the degree of quantization. The polymodality we observe phenomenologically differs from what is commonly reported, e.g., in [5], where the peaks are located at integer multiples with amplitude decay, as a result of the phase preference when the external force is applied. The mechanism we propose provides various forms of interspike interval distribution, thus offering a potential explanation for the fact that the modes in the polymodal distributions of generation times observed experimentally are not equal to an integer times a quantal period [2].

We study for this purpose a population of coupled synthetic genetic relaxation oscillators, mainly for the following reasons. (i) The constructed synthetic networks have a rather simple topology with an exactly known structure, in contrast to the presently investigated circadian oscillator models. (ii) The construction of synthetic genetic networks, using mutually activating or repressing genes (or gene products), enables engineers to evolve biological systems by means of variation and selection for any function they desire, mimicking cell behavior. The design of these synthetic "applets," experimentally realized in simple organisms such as *Escherichia coli* and yeast, is significant not only for the synthesis of artificial biological systems, but also for biotechnological and therapeutic applications [10,11].

The majority of experimentally constructed synthetic genetic networks can exhibit bistable [12] or oscillatory behavior [13,14] when in isolation. It has been shown theoretically, however, that when organized in a population they can achieve synchronization, if appropriate mechanisms of coupling are present. These mechanisms require intercell communication, such as the quorum sensing mechanism, used, e.g., in *Vibrio fischeri*, a bioluminescent bacterium that colonizes the light organs of certain marine species [15]. This mechanism relies on the exchange of small signaling molecules, known as the autoinducers (AIs), which diffuse through the cell membrane and are thereby shared by all cells in the population. Therefore, the *V. fischeri* LuxIR complex has been proposed as an adequate method to obtain synchronization of isolated genetic units [16,17]. However, the same type of interaction between cells can generate additional stable regimes, e.g., the oscillation death (OD) regime known also as the inhomogeneous steady state [18], if the coupling between the oscillators is sufficiently large. Recently, we have shown [19] that this type of coupling inherently leads to multistability (existence of many different modes of organized collective behavior) and multirhythmicity in a model of genetic relaxation oscillators [18].

Here, we show that the presence of multistability strongly influences the response of the system to different external stimuli, such as the effects of extrinsic and intrinsic noise on a particular model. Physically, this type of noise can be generated by an external field, e.g., an electromagnetic field [20], and its levels can be manipulated experimentally [21]. We demonstrate that the effects of quantized cycling in a system of globally coupled synthetic genetic oscillators can be induced by the interplay of intercell signaling and sto-

chasticity. We show also how inhomogeneity can be used to enhance the quantizing effect in such systems, while by changing the noise intensity or an adequate parameter one can manipulate the degree of polymodality in the system. Furthermore, for an optimal value of the noise amplitude, maximal variability in the system can be obtained.

The underlying genetic circuitry of the model we consider [18] is a hysteresis-based genetic relaxation oscillator, constructed from a toggle switch composed of two genes u and v that inhibit each other, and a quorum sensing mechanism which, on one hand, provides the transition from trigger to limit cycle in a single cell, and also by diffusing AI molecules through the cell membrane, enables coupling in the network (details are given in [18]). The time evolution of the system is governed by the dimensionless equations.

$$\frac{du_i}{dt} = \alpha_1 f(v_i) - u_i + \alpha_3 h(\omega_i), \tag{1}$$

$$\frac{dv_i}{dt} = \alpha_2 g(u_i) - v_i, \tag{2}$$

$$\frac{d\omega_i}{dt} = \varepsilon[\alpha_4 g(u_i) - \omega_i] + 2d(\omega_e - \omega_i) + \xi_i(t), \tag{3}$$

$$\frac{d\omega_e}{dt} = \frac{d_e}{N}\sum_{i=1}^{N}(\omega_i - \omega_e). \tag{4}$$

where N denotes the total number of cells (oscillators), and w_i represents the intracellular, and w_e the extracellular AI concentration. The mutual influence of the genes is carried out through the functions $f(v)=1/(1+v^{\beta})$, $g(u)=1/(1+u^{\gamma})$, and $h(w)=w^{\eta}/(1+w^{\eta})$, where β, η, and γ are the parameters of the corresponding activatory or inhibitory Hill functions. The dimensionless parameters α_1 and α_2 determine the expression strength of the toggle switch genes, α_3, the activation due to the AI, and α_4, the repressing of the AI. The coupling coefficients in the system, d and d_e (intracellular and extracellular), depend mainly on the diffusion properties of the membrane [18]. One of the main characteristics of this model is the presence of multiple time scales, producing relaxation oscillations. The noise term $\xi_i(t)$ models the contribution of random fluctuations and is a Gaussian white noise with zero mean. We assume that the deterministic equations provide a reasonable description of the system's dynamics, whereas the noise term represents the inevitable fluctuations in living systems. It is considered that the noise intensity σ_a^2 is rather small, not exceeding the order of 10^{-6}; hence, a sufficient motivation to use Gaussian noise and Langevin equations. The numerical integrations are performed using standard techniques for stochastic differential equations [22].

A detailed analysis of the deterministic model of identical, globally coupled relaxation genetic oscillators Eqs. (1)–(4) has revealed multistability—the appearance of several coexisting dynamical regimes (in-phase, antiphase, and asymmetric oscillations and the OD regime), as well as the ability of the system to produce clustering and multiple rhythms (note the different period values for various attractors) [19], as a result of the inhibitory, phase-repulsive coupling present. The solution to which we refer as asymmetric oscillations [Fig. 1(a)] is characterized by the presence of large- and small-amplitude oscillations in one attractor: one of the oscillators performs large excursions, while the other one oscillates in the vicinity of the steady state [19].

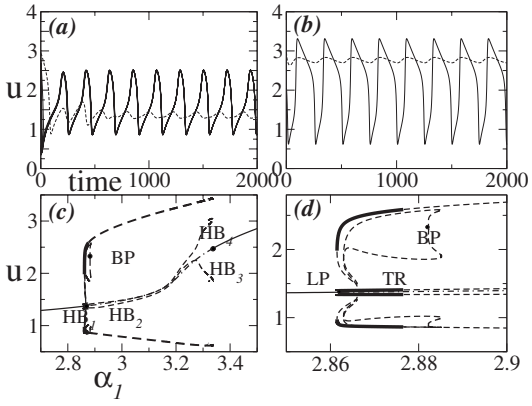

FIG. 1. (a) Asymmetric solution when eight identical oscillators are organized in two oscillatory clusters. The distribution of the oscillators between the clusters is 1:7 (period $T=216.95$) for $\alpha_1=2.868$, $\alpha_2=5$, $\alpha_3=1$, $\alpha_4=4$, $\beta=\gamma=\eta=2$, $\varepsilon=0.01$, $d=0.001$, and $d_e=1$. (b) Distribution 4:4 ($T=249.43$) for nonidentical elements with α_1 values between 3.246 and 3.4. (c) Bifurcation diagram obtained for two identical oscillators by variation of α_1. The asymmetric solution lies on a secondary unstable bifurcation branch, started from a pitchfork bifurcation point BP. The one-parameter continuation moves in the direction of the *subcritical Hopf bifurcation* HB_1, where the asymmetric regime gains stability between a saddle node (LP) and a torus bifurcation (TR) (d), the latter ensuring the presence of two frequencies in the system. (d) Detailed view of the region where stable asymmetric oscillations exist. Thin solid lines denote stable steady state, thick solid lines, the stable limit cycle, dash-dotted lines, the unstable steady state, and dotted lines the unstable limit cycle.

In this work, however, we focus mainly on the behavior of the system when the elements are nonidentical, i.e., more realistically describing real networks. The heterogeneity is achieved by introducing certain diversity in the α_1 parameter values, not greater than 4% in separate elements. Thus, we study the case when all oscillators are confined to the oscillatory region. A bifurcation analysis performed on a system of two slightly nonidentical elements shows a significant enlargement of the parametric area where the asymmetric solution is stable with respect to the equivalent investigations for identical elements [19] [compare Figs. 2(a) and 2(b) and 1(c) and 1(d)]. For illustration, the asymmetric solution now consists of two separate branches: the first one, emerging from HB_1 (HB_3) [Fig. 2(a)], characterizes small-amplitude oscillations around the lower stable state [Fig. 1(a)], whereas the second branch [Fig. 2(b)] emerging from HB_2 (HB_4) is characterized by small-amplitude oscillations around the upper stable state [Fig. 1(b)]. The stability regions depend mainly on the degree of the system's heterogeneity: larger diversity between the elements leads to a larger parametric region of stability. Note that in this case the asymmetric solution arises directly from the HB, whereas for identical elements, it is

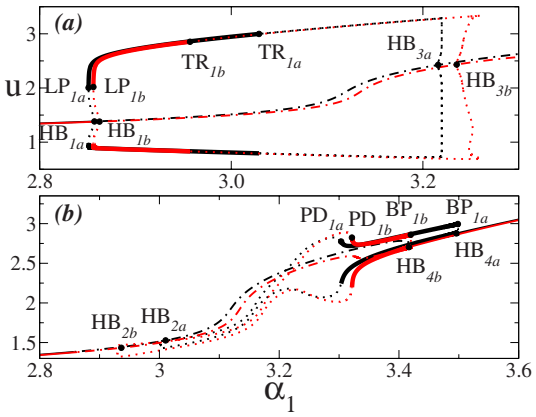

FIG. 2. (Color online) Bifurcation analysis for two nonidentical elements. The parametric region of stability of the asymmetric solution is enlarged when the divergence between the two elements is greater: compare the black thick line (difference between the α_1 values of the two elements is 4%) and the gray (red) thick line (difference between the α_1 values is 2%). For line notation refer to Fig. 1.

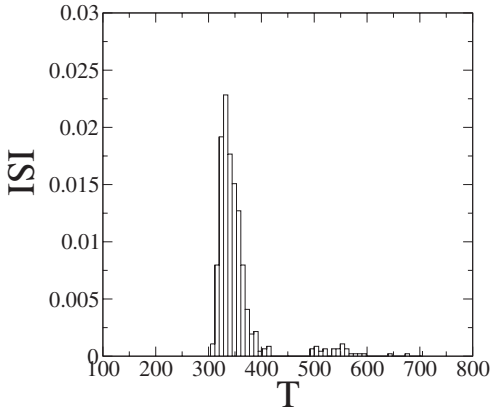

FIG. 3. Multimodal distribution of the ISIs for isolated oscillator, when $\alpha_1=3.328$ and $\sigma_a^2=7\times10^{-7}$.

necessary first to identify the broken-symmetry BP.

The manifestation of the specific coupling present in the system can be extracted from the bifurcation analysis and the numerical simulations performed: a strong reduction in the system's dimension is established as a result of the clustering that occurs. Thus, the two cluster decompositions are determined as most probable, with the possibility for different distributions of the oscillators between the clusters, each characterized by different periods of oscillations [Figs. 1(a) and 1(b)] (some of them consisting of a sequence of several subperiods [19]). Therefore, complex dynamical behavior can be predicted in the presence of noise, identifying the interplay with heterogeneity and intercell coupling as critical at this point. In order to determine the effective jumps of the oscillators in the system due to noise, we analyze statistically the interspike intervals (ISIs) called also the frequency distribution [2]. Starting with the noise-free case, an autooscillatory solution is obtained for a single oscillator ($T=336.84$), when α_1 is fixed to a value slightly before α_{1HB_3}. Including the noise term, however, leads to a multipeak distribution of the ISIs, although only slightly noticeable (Fig. 3) (similar examples of noise effects in the vicinity of subcritical HBs are known in the literature [23]).

Now, we consider a population of identical genetic units, whose dynamics is significantly influenced by the specific type of cell-cell communication. We find that the noise in this case contributes to the establishment of variability and the well-expressed presence of multiple frequencies [see Figs. 4(a) and 4(b)], despite the initially synchronized behavior of the identical elements. The cycling is now quantized, having either almost bimodal [obtained for $\alpha_1=3.3$ Fig. 4(a)] or polymodal [$\alpha_1=3.328$, Fig. 4(b)] solutions. Choosing slightly different α_1 values, one can effectively switch between different multipeak distributions, adapting the artificial network to produce the desired frequencies. In order to identify the underlying mechanism responsible for various polymodal distributions of generation times, it is important to note that, in the presence of noise, we cannot speak about switching between different attractors, because they are not very deterministic and their lifetimes are rather short. Therefore, a one-to-one correspondence between the deterministic and stochastic attractors cannot be established. However, the distribution of the probability density to find phase points near the jumping threshold is mainly controlled by the presence of attractors found by the bifurcation analysis above and in [19], and this density determines the ISI peaks observed. The modes in the polymodal histogram might be separated by almost equal intervals if one of the stochastic attractors dominates or by different intervals in the opposite case. The same interplay between attractors disrupts the exponential decay of the peak amplitudes, which is typical for a noisy attractor under the influence of a periodic signal [6].

Furthermore, the variability is significantly enhanced when the network becomes slightly inhomogeneous and noise is present (Fig. 5). Slight manipulations of the α_1 values even allow switching between the unimodal, bimodal, and polymodal solutions obtained. Another important effect we report here is the possibility to observe maximal variability in the system for an optimal noise intensity. This is in contrast to the well-known effect of coherence resonance [24], where, for intermediate noise intensities, maximal order could be achieved in systems with underlying nonlinear dynamics [25]. The results also show that, although organized in a population, different oscillators are characterized by different ISI distributions, as a consequence of the specific, repulsive coupling considered.

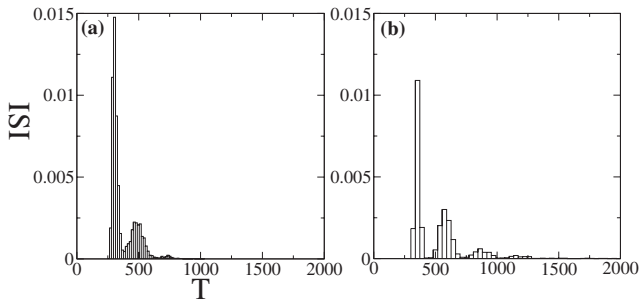

FIG. 4. (a) Bimodal ISI distribution for eight identical oscillators ($\alpha_1=3.3$) and (b) polymodal ISI distribution ($\alpha_1=3.328$). The noise intensity is $\sigma_a^2=5\times10^{-7}$.

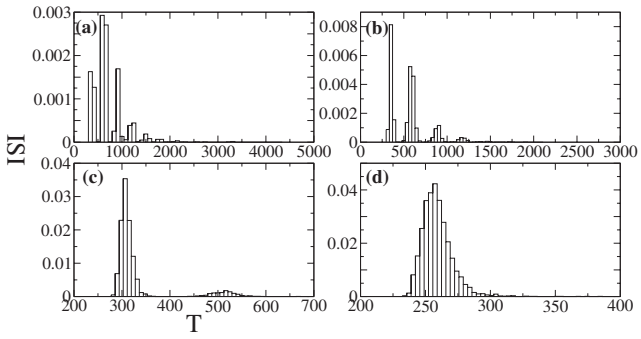

FIG. 5. Variability in the ISIs for four nonidentical elements (from an eight-element network): multimodal for (a) $\alpha_1=3.328$ and (b) $\alpha_1=3.325$, bimodal for (c) $\alpha_1=3.31$, and unimodal for (d) $\alpha_1=3.25$. The noise intensity is $\sigma_a^2=5\times10^{-7}$.

In summary, we have proposed a mechanism for quantized cycling in artificial gene networks, based on the interplay of cell-to-cell communications and stochasticity. This mechanism allows quantized generation time in an oscillatory population, despite the previous findings, where quantized cycles were observed mainly for an isolated oscillator. The variability obtained can be thus manipulated with only one control parameter, which allows a precise switching between different polymodal distributions. Therefore, the functionality of the artificial genetic unit in a large set of frequencies can be considered as a significant advantage in a multitude of applications, such as the constructions of biochips, the "new era" of drug production, cellular control, etc. Moreover, the effects reported here might provide insight into the treatment strategies of the so-called dynamical diseases [26]. Considering the temporal dimension of illness, it will be of certain importance whether the therapeutic applications exhibit complex behavior. We hope that, due to the simplicity of the genetic motifs considered here, these findings will also contribute to the understanding of naturally produced cell time quantization. It would also be interesting to compare this mechanism with other possible sources of quantization, e.g., noise and multistability in genetic networks with delay [27].

A. K. acknowledges the International Max Planck Research School on Biomimetic Systems, E. V the DFG (SFB 555) and the program "Radiofizika" of the Russian Academy of Sciences (Grant No. RFBR-05-02-16518-a), A. Z. the Volkswagen-Stiftung, CESCA-CEPBA, and J. K. the EU through the Network of Excellence "BioSim," Contract No. LSHB-CT-2004-005137.

[1] D. Lloyd and E. I. Volkov, BioSystems **23**, 305 (1990).
[2] R. R. Klevecz, Proc. Natl. Acad. Sci. U.S.A. **73**, 4012 (1976).
[3] A. Sveiczer *et al.*, J. Cell. Sci. **109**, 2947 (1996).
[4] Y. Masui and P. Wang, Biol. Cell **90**, 537 (1998).
[5] V. A. Makarov, V. I. Nekorkin, and M. G. Velarde, Phys. Rev. Lett. **86**, 3431 (2001).
[6] A. Longtin, Chaos **5**, 209 (1995).
[7] L. Gammaitoni, P. Hänggi, P. Jung, and F. Marchesoni, Rev. Mod. Phys. **70**, 223 (1998).
[8] A. Sveiczer *et al.*, Proc. Natl. Acad. Sci. U.S.A. **97**, 7865 (2000).
[9] R. Steuer, J. Theor. Biol. **228**, 293 (2004).
[10] J. Hasty, F. Isaacs, M. Dolnik, D. McMillen, and J. J. Collins, Chaos **11**, 207 (2001).
[11] J. Hasty, D. McMillen, and J. J. Collins, Nature (London) **420**, 224 (2002).
[12] T. S. Gardner, C. R. Cantor, and J. J. Collins, Nature (London) **403**, 339 (2000).
[13] M. B. Elowitz and S. Leibler, Nature (London) **403**, 335 (2000).
[14] N. Atkinson, M. Savagean, J. Myers, and A. Ninfa, Cell **113**, 597 (2003).
[15] C. Fuqua and P. Greenberg, Nat. Rev. Mol. Cell Biol. **3**, 685 (2002).
[16] J. García-Ojalvo, M. Elowitz, and S. Strogatz, Proc. Natl. Acad. Sci. U.S.A. **101**, 10955 (2004).
[17] D. McMillen, N. Kopell, J. Hasty, and J. J. Collins, Proc. Natl. Acad. Sci. U.S.A. **99**, 679 (2002).
[18] A. Kuznetsov, M. Kern, and N. Kopell, SIAM J. Appl. Math. **65**, 392 (2005).
[19] A. Koseska, E. Volkov, A. Zaikin, and J. Kurths, Phys. Rev. E **75**, 031916 (2007).
[20] J. Hasty, J. Pradines, M. Dolnik, and J. J. Collins, Proc. Natl. Acad. Sci. U.S.A. **97**, 2075 (2000).
[21] W. J. Blake, M. Kaern, C. R. Cantor, and J. J. Collins, Nature (London) **422**, 633 (2003).
[22] J. García-Ojalvo and J. M. Sancho, *Noise in Spatially Extended Systems*, (Springer, New York, 1999).
[23] O. V. Ushakov *et al.*, Phys. Rev. Lett. **95**, 123903 (2005).
[24] A. S. Pikovsky and J. Kurths, Phys. Rev. Lett. **78**, 775 (1997).
[25] A. Koseska, A. Zaikin, J. García-Ojalvo, and J. Kurths, Phys. Rev. E **75**, 031917 (2007).
[26] J. Blair, L. Glass, U. an der Heiden, and J. Milton, *Dynamical Disease: Mathematical Analysis of Human Illness* (AIP, Woodbury, NY, 1995).
[27] S. A. Campbell, J. Bélair, T. Ohira, and J. Milton, Chaos **5**, 640 (1995); D. A. Bratsun, D. N. Volfson, L. S. Tsimring, and J. Hasty, Proc. Natl. Acad. Sci. U.S.A. **102**, 14593 (2005).